JPEDAV (2005) 26:579-590
DOI: 10.1361/154770305X74377
1547-7037/$19.00 ©ASM International

Determination and Assessment of Ternary Interdiffusion Coefficients from Individual Diffusion Couples

Kevin M. Day, L.R. Ram-Mohan, and Mysore A. Dayananda

(Submitted June 3, 2005; in revised form September 20, 2005)

Two pairs of diffusion couples were assembled with α (fcc) Cu-Ni-Zn alloys characterized by similar thermodynamic activities for Cu and annealed at 775 °C. One pair of couples exhibited intersecting diffusion paths, and the other pair showed overlapping path segments. They were analyzed for interdiffusion fluxes, zero-flux-planes, and ternary interdiffusion coefficients directly from the concentration profiles. The analysis was based on converting profiles of concentrations to profiles of interdiffusion fluxes and evaluating moments of interdiffusion fluxes for the determination of interdiffusion coefficients over selected composition ranges. For the pair with intersecting diffusion paths, ternary interdiffusion coefficients were determined from the individual couples in the region of their common composition; these coefficients were in agreement with each other and with those determined by the Boltzmann-Matano analysis. For the pair of couples with overlapping diffusion path segments, interdiffusion coefficients calculated from each couple over the common path segment agreed with each other. In addition, the interdiffusion coefficients calculated over various composition regions were used to regenerate the concentration profiles of the individual couples. All calculations were carried out with the aid of a computer program called *Multi*DiFlux, which was developed by Dayananda and Ram-Mohan as a free educational and research tool for analysis of multicomponent diffusion.

1. Introduction

Interdiffusion in an n-component system can be described by Onsager's formalism of Fick's law where $(n - 1)^2$ interdiffusion coefficients are defined as functions of composition.[1] For ternary systems, four composition-dependent interdiffusion coefficients are needed. The classic method used to calculate the four coefficients is the Boltzmann-Matano analysis, which requires two independent diffusion couples with intersecting diffusion paths; ternary interdiffusion coefficients are evaluated at the common composition of the couple pair.[1] Dayananda and Sohn[2] proposed an alternative method, where the four ternary interdiffusion coefficients are calculated from a single diffusion couple over selected composition ranges along the diffusion path. In this method, the calculated interdiffusion coefficients are treated as average values over the selected composition ranges.

The purpose of this paper is to analyze selected diffusion couples investigated in the Cu-Ni-Zn system at 775 °C[3,4] for the determination of interdiffusion fluxes, zero-flux-planes (ZFP), and ternary interdiffusion coefficients over various concentration ranges within the diffusion zone. For such analysis, a user-friendly computer program called *Multi*DiFlux was developed as a research and teaching tool by Dayananda and Ram-Mohan,[5] utilizing the methodology of Dayananda[6] and Dayananda and Sohn.[2] The diffusion couples analyzed in this paper were characterized by terminal alloys with similar thermodynamic activity for Cu. A pair of such Cu-isoactivity couples with intersecting diffusion paths was selected for the evaluation of the ternary interdiffusion coefficients independently from each couple in the region of the common composition of the intersection. Such analysis would allow a comparison of the interdiffusion coefficients calculated by the Boltzmann-Matano analysis at the common composition with those evaluated from the individual couples by the *Multi*Diflux program.[7] In addition, two other Cu-isoactivity couples, characterized by similar segments in their diffusion paths, were also selected for evaluation and assessment of the interdiffusion coefficients calculated with the aid of the *Multi*DiFlux program.

The *Multi*DiFlux program is also assessed for accuracy in the calculated ternary interdiffusion coefficients by applying it to concentration profiles theoretically generated on the basis of error function solutions[1,7] for a test ternary diffusion couple[2] characterized by a set of constant interdiffusion coefficients. The interdiffusion coefficients evaluated by the program from such concentration profiles are compared with the original set of interdiffusion coefficients initially used to generate the profiles.

2. Experimental Procedure

The various Cu-Ni-Zn diffusion couples examined in this study were assembled and annealed by Dayananda and Kim.[3,4] The alloys used for the couples were prepared from oxygen-free-high-conductivity (OFHC) copper, high-purity nickel, and high-purity zinc by induction melting in alumina crucibles under an argon atmosphere. The melts were allowed to solidify into ingots in the alumina crucibles, cold rolled to 10% reduction, and given a homogenizing

Kevin M. Day and **Mysore A. Dayananda,** School of Materials Engineering, Purdue University, West Lafayette, IN 47907-2044; and **L.R. Ram-Mohan,** Quantum Semiconductor Algorithms, Northborough, MA 01532. Contact e-mail: dayanand@ecn.purdue.edu.

anneal for one week at 900 °C. The compositions of the alloys are listed in Table 1 and are shown on a Cu-Ni-Zn ternary isotherm in Fig. 1. Also drawn in Fig. 1 are a few iso-activity lines for Cu based on thermodynamic calculations carried out by Sisson and Dayananda[8] from Gibbs-Duhem integration and experimental thermodynamic data for binary and ternary alloys in the Cu-Ni-Zn system. The various couples examined in this study are: α_2 versus α_7, α_{10} versus α_{13}, α_3 versus α_{15}, and α_3 versus α_{18}. These couples are referred to as Cu-isoactivity couples, as the terminal alloys of the couples lie on a Cu-isoactivity line. It has been shown experimentally by Dayananda and coworkers[3,4,6,9] that when the terminal alloys of a diffusion couple are located on an isoactivity line of a selected component, a zero-flux-plane (ZFP) for that component will develop in the diffusion zone.

Diffusion couples were assembled by cutting the alloy ingots into diffusion disks and metallographically polishing the surfaces of the disks through 0.05 μm alumina. Selected disks were then clamped together in a Kovar jig to make a diffusion couple. All of the couples were placed in quartz tubes, which were flushed with hydrogen, evacuated to less then 1.0 pascal, and sealed. Couples were annealed for two days at 775 °C in a Lindberg heavy-duty three-zone tube furnace (Asheville, NC). Following the diffusion anneal, the couples were quenched to preserve the high-temperature microstructure. Diffused couples were mounted and cut to reveal a section parallel to the diffusion direction. Each couple was metallographically polished and etched with a potassium dichromate solution[10] to reveal the diffusion structure.

Concentration profiles of Zn, Ni, and Cu were determined for the various couples by employing a point-to-point counting technique with a Cameca SX-50 microprobe (Cedex, France) equipped with wavelength dispersive spectrometers. The intensities of the K_α x-radiation peaks of Zn, Ni, and Cu were measured at various points in the diffusion zone along traces parallel to the diffusion direction and were converted to compositions by using elemental standards and a Z = atomic member; A = absorption; F = fluorescence (ZAF) correction program.

The experimental concentration profiles are analyzed in this study by employing the *Multi*DiFlux program for the determination of the interdiffusion fluxes of all components over the entire diffusion zone and the calculation of the ternary interdiffusion coefficients over selected composition ranges along the diffusion path.

Table 1 Selected single phase alloy compositions

	Composition, at.%		
Alloy	Cu	Ni	Zn
α_2	73.5	8.4	18.1
α_3	59.3	13.3	27.4
α_7	56.4	43.6	0.0
α_{10}	80.0	0.0	20.0
α_{13}	62.8	37.2	0.0
α_{15}	24.6	75.4	0.0
α_{18}	35.4	51.6	13.0

3. Determination of Ternary Interdiffusion Coefficients

Based upon Onsager's formalism of Fick's law,[11] the interdiffusion flux $\tilde{J}_i$ of component i in a ternary system can be expressed in terms of two independent concentration gradients:

$$\tilde{J}_i = -\tilde{D}^3_{i1}\frac{\partial C_1}{\partial x} - \tilde{D}^3_{i2}\frac{\partial C_2}{\partial x} \quad (i = 1,2) \qquad \text{(Eq 1)}$$

where $\tilde{D}^3_{i1}$ and $\tilde{D}^3_{i2}$ (i = 1,2) are the four ternary interdiffusion coefficients.

The interdiffusion fluxes for each of the components can be determined directly from their concentration profiles without the need for interdiffusion coefficients.[3,4,6,9] The

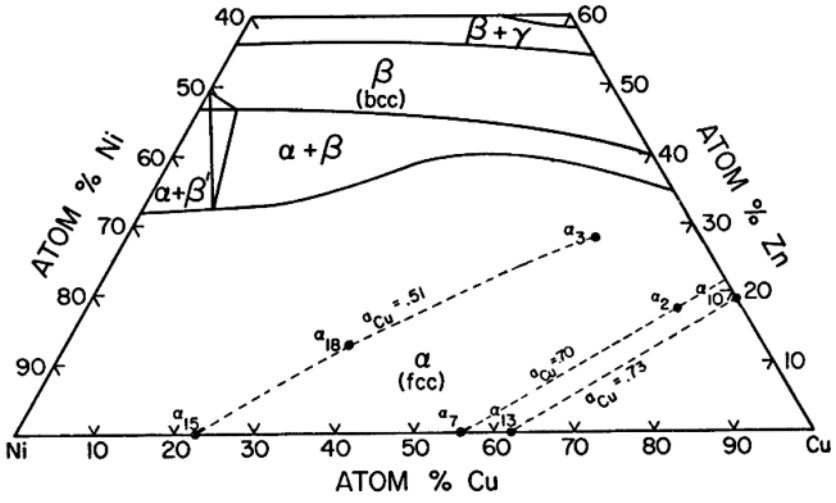

Fig. 1 Alloys used for the couples are identified on the Cu-Ni-Zn ternary isotherm at 775 °C.[4] The dashed lines indicate the Cu isoactivity lines[8] passing through the various terminal alloys. The thermodynamic activity (a_{Cu}) of Cu is based on pure Cu as the standard state.

interdiffusion flux for each component can be calculated directly from the concentration profile at any section x from the relation[3,6]:

$$\tilde{J}_i = \frac{1}{2t} \int_{C_i^- \text{ or } C_i^+}^{C_i(x)} (x - x_o)\mathrm{d}C_i \quad (i = 1,2, \ldots, n) \qquad \text{(Eq 2)}$$

where t is the time in seconds, C_i^- and C_i^+ are the terminal compositions, and x_o is the location of the Matano plane. The molar volume is normally considered to vary little within the diffusion zone. For diffusion couples, where the variation in molar volume cannot be ignored, Eq 2 can be modified[6]:

$$\tilde{J}_i(x^*) = \frac{(C_i^- - C_i^+)}{2t}\left[Y_i^* \int_{-\infty}^{x^*} \frac{(1 - Y_i)}{V_m}\,\mathrm{d}x + (1 - Y_i^*) \int_{x^*}^{+\infty} \frac{Y_i}{V_m}\,\mathrm{d}x \right] \quad (i = 1,2 \ldots, n) \qquad \text{(Eq 3)}$$

where

$$Y_i = \frac{C_i - C_i^+}{C_i^- - C_i^+} \quad (i = 1,2 \ldots, n) \qquad \text{(Eq 4)}$$

and V_m is the molar volume. For a system with negligible variation in molar volume, V_m in Eq 3 can be set to 1, if the concentrations are expressed in atom fractions. The fluxes are then in the units of atom fraction μm/s but can be converted to moles/μm^2/s by multiplying with the actual molar density. The use of Eq 3 for calculating the interdiffusion fluxes has the advantage of bypassing the need to determine the location of the Matano plane.

The interdiffusion flux determined from Eq 2 or Eq 3 can be integrated over a selected region, x_1 to x_2. Hence, on the basis of Eq 1 one obtains[2]:

$$\int_{x_1}^{x_2} \tilde{J}_i \mathrm{d}x = -\int_{C_1(x_1)}^{C_1(x_2)} \tilde{D}_{i1}^3 \mathrm{d}C_1 - \int_{C_2(x_1)}^{C_2(x_2)} \tilde{D}_{i2}^3 \mathrm{d}C_2 \quad (i = 1,2)$$
$$= \overline{\tilde{D}}_{i1}^3 [C_1(x_1) - C_1(x_2)] + \overline{\tilde{D}}_{i2}^3 [C_2(x_1) - C_2(x_2)] \; (i = 1,2) \qquad \text{(Eq 5)}$$

where $\overline{\tilde{D}}_{i1}^3$ and $\overline{\tilde{D}}_{i2}^3$ are the average values of the interdiffusion coefficients over the composition range along the diffusion path between $C_i(x_1)$ to $C_i(x_2)$. The average interdiffusion coefficients are defined[2]:

$$\overline{\tilde{D}}_{ij}^3 = \int_{C_j(x_1)}^{C_j(x_2)} \tilde{D}_{ij}^3 \mathrm{d}C_j \Big/ \int_{C_j(x_1)}^{C_j(x_2)} \mathrm{d}C_j \quad (i = 1,2) \qquad \text{(Eq 6)}$$

Because the values of $\overline{\tilde{D}}_{ij}^3$ are characteristic of the diffusion path, as defined in Eq 6, they can be treated as constants over the selected composition range, and Eq 1 can be modified:

$$\tilde{J}_i = -\overline{\tilde{D}}_{i1}^3 \frac{\partial C_1}{\partial x} - \overline{\tilde{D}}_{i2}^3 \frac{\partial C_2}{\partial x} \quad (i = 1,2) \qquad \text{(Eq 7)}$$

If both sides of Eq 7 are multiplied by $(x - x_o)^n$, where n is an integer, and integrated between x_1 and x_2 in the diffusion zone[2]:

$$\int_{x_1}^{x_2} \tilde{J}_i (x - x_o)^n \mathrm{d}x = -\overline{\tilde{D}}_{i1}^3 \int_{C_1(x_1)}^{C_1(x_2)} (x - x_o)^n \mathrm{d}C_1 - \overline{\tilde{D}}_{i2}^3 \int_{C_2(x_1)}^{C_2(x_2)} (x - x_o)^n \mathrm{d}C_2 \quad (i = 1,2) \qquad \text{(Eq 8)}$$

For $n = 1$, Eq 8 becomes:

$$\int_{x_1}^{x_2} \tilde{J}_i (x - x_o)\mathrm{d}x = -\overline{\tilde{D}}_{i1}^3 \int_{C_1(x_1)}^{C_1(x_2)} (x - x_o)\mathrm{d}C_1 - \overline{\tilde{D}}_{i2}^3 \int_{C_2(x_1)}^{C_2(x_2)} (x - x_o)\mathrm{d}C_2 = 2t\{\overline{\tilde{D}}_{i1}^3 [\tilde{J}_1(x_1) - \tilde{J}_1(x_2)] + \overline{\tilde{D}}_{i2}^3 [\tilde{J}_2(x_1) - \tilde{J}_2(x_2)]\} \; (i = 1,2) \qquad \text{(Eq 9)}$$

in light of Eq 2.

Equations 5 and 9 provide four equations involving the four interdiffusion coefficients, $\overline{\tilde{D}}_{11}^3$, $\overline{\tilde{D}}_{12}^3$, $\overline{\tilde{D}}_{21}^3$, $\overline{\tilde{D}}_{22}^3$. By setting up and solving Eq 5 and 9 over selected composition ranges in the diffusion zone, all four interdiffusion coefficients can be calculated from a single diffusion couple. This analysis is used by the *Multi*DiFlux program for the calculation of ternary interdiffusion coefficients.

4. Details of the *Multi*DiFlux Program

The *Multi*DiFlux program employs several successive steps in the analysis of experimental data for a diffusion couple. These steps are described below.

4.1 Interpolation of Experimental Concentration Profiles

The first step in the analysis by the *Multi*DiFlux program is to fit the experimental data on concentration profiles with cubic Hermite interpolation polynomials by the method of least squares developed by Ram-Mohan.[12] The fitting routine allows the user to break up a concentration profile into several "regions" as specified by the user. The compositions at the endpoints of a region correspond to the experimental data and the derivatives of concentrations at the endpoints of the region are calculated by the *Multi*DiFlux program based on the cubic Hermite polynomial fitting of the data in the region. The fitting routine ensures continuity in both concentrations and their derivatives at both ends of all regions. In addition, the user has the flexibility of specifying values for concentration derivatives at any end point of a region. This control over the derivatives at the endpoints of a region allows the user to set them to zero at the terminal regions and at the locations of maxima or minima in concentration profiles.

Each region can be further divided into subregions of equal length called "elements" based on the user's choice

for improved interpolation of the profile segments that have appreciable variation in curvature. By appropriate choice of regions and elements, a concentration profile with considerable variation in curvature and with maxima and minima can be satisfactorily fitted with cubic Hermite interpolation polynomials.

4.2 Matano Plane Determination

The second step performed by the *Multi*DiFlux program is to calculate the location of the Matano plane from the fitted profile of each component. The location of the Matano plane is determined on the basis of mass balance for each component by the following relation:

$$\int_{x^-}^{x^+} C_i \mathrm{d}x = (x_{o,i} - x^-)(C_i^- - C_i^+) \quad (i = 1,2,3) \qquad \text{(Eq 10)}$$

where $x_{o,i}$ is the Matano plane location for component i, and x^- and x^+ are the x coordinates for the extreme left and extreme right of the diffusion zone.

From the concentration profile of each component, the program calculates the $x_{o,i}$ location of the Matano plane. These $x_{o,i}$ values normally differ little for systems with little variation in molar volume within the diffusion zone. Large differences in the calculated Matano plane locations from the individual components suggest that the molar volume in the diffusion zone is appreciable and must be taken into account in Eq 3. Incomplete data for concentration profiles can also yield dissimilar Matano plane locations for the individual components.

4.3 Calculation of Interdiffusion Fluxes

The third step for the program is to calculate the interdiffusion flux $\tilde{J}_i$ of each component from the interpolated profiles, employing Eq 2 or 3, and to provide output to generate plots of $\tilde{J}_i$ as a function of x.

4.4 Calculation of Interdiffusion Coefficients

The fourth step performed by the *Multi*DiFlux program is to calculate a set of ternary interdiffusion coefficients employing Eq 5 and 9 over each selected composition range within the diffusion zone. The user may start with two regions, one on either side of the Matano plane, as a starting point but can alter the regions and increase their number.

The acceptability of the calculated sets of interdiffusion coefficients over a given region is checked in the next two steps.

4.5 Generation of Concentration Profiles from Interdiffusion Coefficients

The fifth step carried out by the *Multi*DiFlux program is to generate concentration profiles on the basis of ternary interdiffusion coefficients calculated over the various composition regions selected in the diffusion zone. These calculations use error function solutions that are appropriate for a given composition range between x_I and x_{II} and use interdiffusion coefficients for that range. The error function equations for the concentration profiles of C_i (i = 1, 2), between the concentration limits of C_{iI} and C_{iII}[7] are:

$$C_1 = K_1 \left[\frac{\mathrm{erf}\left(\frac{x - x_0}{2\sqrt{u \cdot t}}\right) - \mathrm{erf}\left(\frac{x_I - x_0}{2\sqrt{u \cdot t}}\right)}{\mathrm{erf}\left(\frac{x_{II} - x_0}{2\sqrt{u \cdot t}}\right) - \mathrm{erf}\left(\frac{x_I - x_0}{2\sqrt{u \cdot t}}\right)} \right] + K_2 \left[\frac{\mathrm{erf}\left(\frac{x - x_0}{2\sqrt{v \cdot t}}\right) - \mathrm{erf}\left(\frac{x_I - x_0}{2\sqrt{v \cdot t}}\right)}{\mathrm{erf}\left(\frac{x_{II} - x_0}{2\sqrt{v \cdot t}}\right) - \mathrm{erf}\left(\frac{x_I - x_0}{2\sqrt{v \cdot t}}\right)} \right] + C_{1I} \qquad \text{(Eq 11)}$$

$$C_2 = K_3 \left[\frac{\mathrm{erf}\left(\frac{x - x_0}{2\sqrt{u \cdot t}}\right) - \mathrm{erf}\left(\frac{x_I - x_0}{2\sqrt{u \cdot t}}\right)}{\mathrm{erf}\left(\frac{x_{II} - x_0}{2\sqrt{u \cdot t}}\right) - \mathrm{erf}\left(\frac{x_I - x_0}{2\sqrt{u \cdot t}}\right)} \right] + \mathrm{K}_4 \left[\frac{\mathrm{erf}\left(\frac{x - x_0}{2\sqrt{v \cdot t}}\right) - \mathrm{erf}\left(\frac{x_I - x_0}{2\sqrt{v \cdot t}}\right)}{\mathrm{erf}\left(\frac{x_{II} - x_0}{2\sqrt{v \cdot t}}\right) - \mathrm{erf}\left(\frac{x_I - x_0}{2\sqrt{v \cdot t}}\right)} \right] + C_{2I} \qquad \text{(Eq 12)}$$

$$K_1 = \frac{1}{\tilde{D}} \left[[\bar{\tilde{D}}_{12}^3 (C_{2II} - C_{2I})] - (\bar{\tilde{D}}_{22}^3 - \bar{\tilde{D}}_{11}^3 - \tilde{D}) \left[\frac{C_{1II} - C_{1I}}{2} \right] \right] \qquad \text{(Eq 13)}$$

$$K_2 = \frac{1}{\tilde{D}} \left[[\bar{\tilde{D}}_{12}^3 (C_{2I} - C_{2II})] - (\bar{\tilde{D}}_{22}^3 - \bar{\tilde{D}}_{11}^3 + \tilde{D}) \left[\frac{C_{1I} - C_{1II}}{2} \right] \right] \qquad \text{(Eq 14)}$$

$$K_3 = \frac{1}{\tilde{D}} \left[[\bar{\tilde{D}}_{21}^3 (C_{1II} - C_{1I})] - (\bar{\tilde{D}}_{11}^3 - \bar{\tilde{D}}_{22}^3 - \tilde{D}) \left[\frac{C_{2II} - C_{2I}}{2} \right] \right] \qquad \text{(Eq 15)}$$

$$K_4 = \frac{1}{\tilde{D}} \left[[\bar{\tilde{D}}_{21}^3 (C_{1I} - C_{1II})] - (\bar{\tilde{D}}_{11}^3 - \bar{\tilde{D}}_{22}^3 + \tilde{D}) \left[\frac{C_{2I} - C_{2II}}{2} \right] \right] \qquad \text{(Eq 16)}$$

$$u = \bar{\tilde{D}}_{11}^3 + 0.5\,(\bar{\tilde{D}}_{22}^3 - \bar{\tilde{D}}_{11}^3 + \tilde{D}) \qquad \text{(Eq 17)}$$

$$v = \bar{\tilde{D}}_{22}^3 + 0.5\,(\bar{\tilde{D}}_{11}^3 - \bar{\tilde{D}}_{22}^3 - \tilde{D}) \qquad \text{(Eq 18)}$$

$$\tilde{D} = \sqrt{(\bar{\tilde{D}}_{11}^3 - \bar{\tilde{D}}_{22}^3)^2 + 4\bar{\tilde{D}}_{12}^3 \bar{\tilde{D}}_{21}^3} \qquad \text{(Eq 19)}$$

For the regeneration of the concentration profiles, the user may initially use only two sets of interdiffusion coefficients evaluated for only two regions, one on either side of the Matano plane.

4.6 Generation of Flux Profiles from Interdiffusion Coefficients

The *Multi*DiFlux program also regenerates the flux profiles on the basis of Eq 7, utilizing the ternary interdiffusion coefficients calculated over various composition ranges selected in the diffusion zone. The correspondence between these flux profiles and those determined on the basis of Eq 2 or 3 improves as the number of regions for the calculation of interdiffusion coefficients is increased and the composition range for the individual regions is decreased.

Table 2 Interdiffusion coefficients associated with the hypothetical diffusion couple

	Interdiffusion coefficients $\tilde{D}^3_{ij}$ ($\times 10^{-15}$ m^2/s)			
	$\tilde{D}^3_{11}$	$\tilde{D}^3_{12}$	$\tilde{D}^3_{21}$	$\tilde{D}^3_{22}$
Input values	23.7	8.1	7.4	11.5
Values calculated by *Multi*DiFlux from regions 1 and 2	23.74	8.04	7.45	11.42

The various calculations described here will be illustrated with a diffusion couple in Sec. 6.

5. Assessment of Calculations with a Test Couple

For the assessment of accuracy in the interdiffusion coefficients calculated by the *Multi*DiFlux program, theoretically generated concentration profiles for a ternary test couple[2] characterized by an arbitrarily selected set of constant interdiffusion coefficients were used. The couple is purely hypothetical and has no bearing to any couple in the Cu-Ni-Zn system investigated in this study. The constant interdiffusion coefficients used for the test couple are given in Table 2 and are the same as those used by Dayananda and Sohn for the test couple in their analysis.[2]

The concentration profile data generated for the test couple on the basis of error functions solutions[1] with interdiffusion coefficients listed in Table 2 are shown in Fig. 2(a). The solid lines in Fig. 2(a) are the cubic Hermite interpolation curves fitted by the *Multi*DiFlux program. In

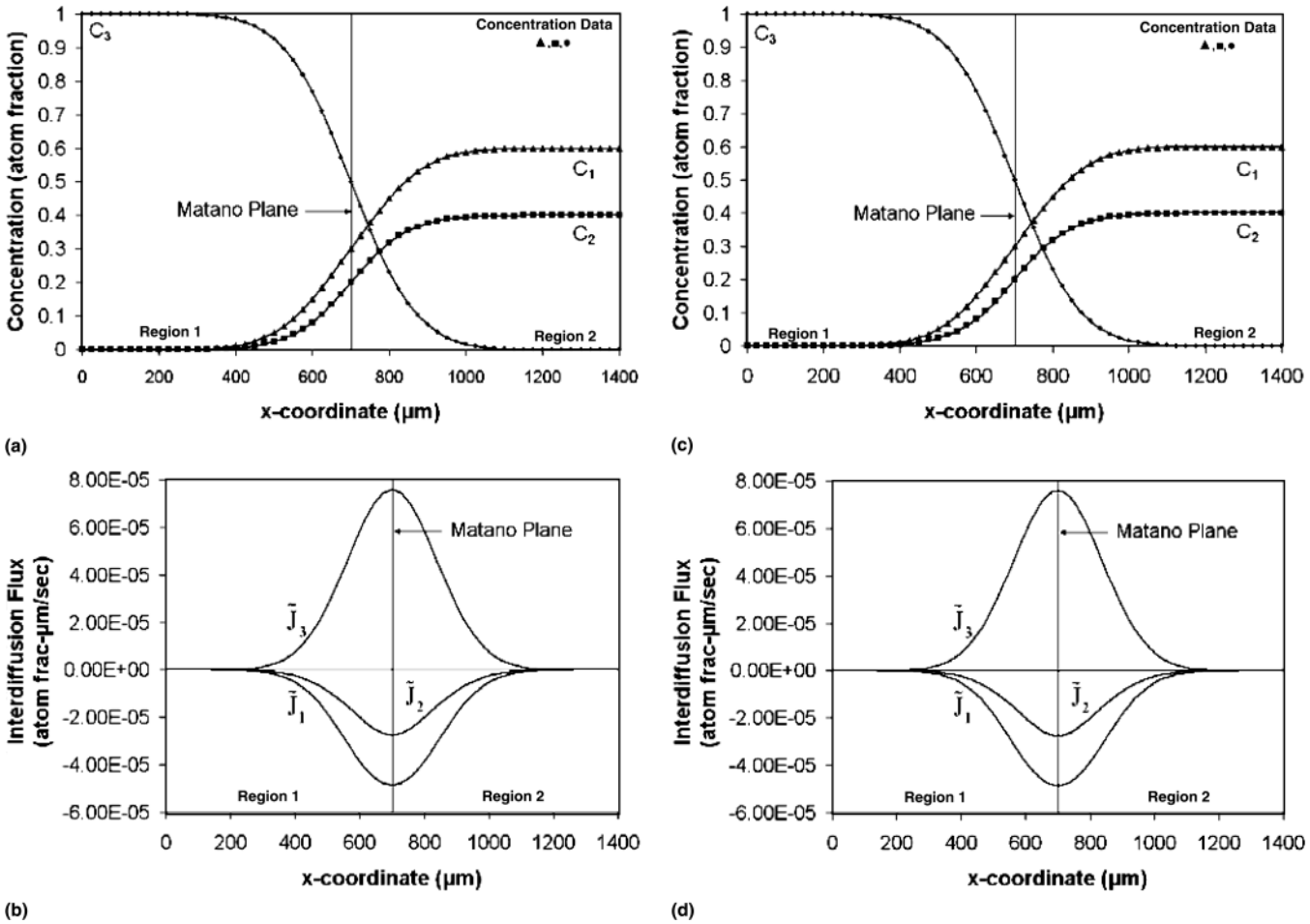

Fig. 2 (a) Concentration profiles for the hypothetical diffusion couple used to assess the *Multi*DiFlux program. The solid lines are the cubic Hermite polynomial curves fitted to the data by the *Multi*DiFlux program. (b) Profiles of interdiffusion fluxes calculated directly from the concentration profiles from Eq 3. (c) Regeneration of the concentration profiles from the calculated interdiffusion coefficients on the basis of error function solutions. (d) Regeneration of the flux profiles from the calculated interdiffusion coefficients on the basis of Eq 7

Fig. 2(b) are presented the interdiffusion fluxes calculated directly from the fitted concentration profiles. The locations of the Matano planes, as determined from the concentration profiles of the three components, are identical (700 μm). The calculated profiles of interdiffusion fluxes for this test couple in Fig. 2(b) are symmetric about the Matano plane, as expected.

To calculate the interdiffusion coefficients for the couple, the concentration profile was divided into two regions, one on either side of the Matano plane, as shown in Fig. 2(a). Interdiffusion coefficients were calculated by the *Multi*DiFlux program for each of these two regions from Eq 5 and 9; they are presented in Table 2. These interdiffusion coefficients are identical for the two regions on either side of the Matano plane and agree with those used to generate the initial concentration profiles within 0.2 to 0.7%. The high accuracy in the calculated interdiffusion coefficients justifies the methodology and analysis described in Sec. 3, as used by the *Multi*DiFlux program. In Fig. 2(c), the concentration profiles regenerated from Eq 11 and 12 are presented on the basis of the calculated interdiffusion coefficients. The excellent reproduction of the concentration profile seen in Fig. 2(c) demonstrates that error function solutions over the selected regions can be conveniently used for the back calculation of the concentration profiles. The flux profiles can also be accurately reproduced from Eq 7 and the calculated interdiffusion coefficients; these profiles are presented in Fig. 2(d). Such reproduction of profiles of concentrations and fluxes serves as a check on the acceptability of the interdiffusion coefficients evaluated by the program. Also, the choice of just two regions used for the calculation of interdiffusion coefficients is more than adequate for the analysis of this couple. However, it should be noted that a single set of interdiffusion coefficients used for this test couple will not be valid in general and for an experimental diffusion couple, several sets of interdiffusion coefficients that are calculated over various regions in the diffusion zone may be required for a full representation and regeneration of the concentration profiles and flux profiles.

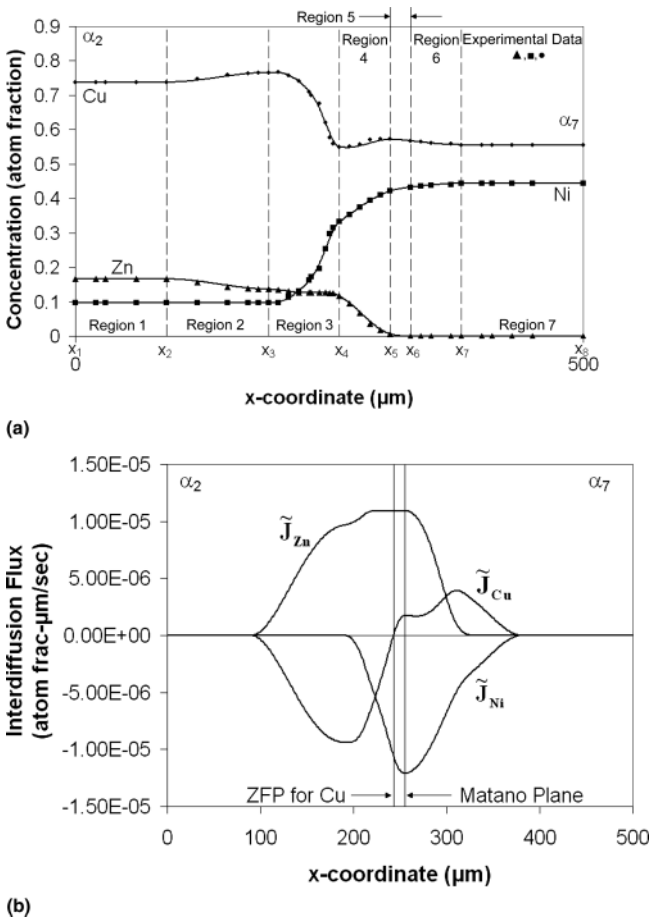

Fig. 3 (a) Concentration profiles for the α_2 versus α_7 diffusion couple divided into seven regions for fitting cubic Hermite interpolation polynomials to the experimental data. The concentrations at the nodal points, x_1, x_2, through x_8 and their derivatives at the endpoints of each of the regions are listed in Table 3. (b) Profiles of interdiffusion fluxes calculated from the fitted concentration profiles

6. Illustration of Use of the *Multi*DiFlux Program

The sequence of steps used by the *Multi*DiFlux program is illustrated with one of the couples assembled with alloys α_2 and α_7, as identified in Fig. 1. The experimental data for the concentration profiles are presented in Fig. 3(a), and the solid lines show the cubic Hermite polynomial curves fitted by the *Multi*DiFlux program. The couple exhibits two relative maxima in Cu concentration, one on either side of the Matano plane as well as a relative minimum in Cu concentration. To fit Hermite polynomials to the experimental data, the diffusion zone was divided into seven regions as marked on Fig. 3(a). The seven regions were selected by choosing the nodal points, x_1 through x_8, at the terminal regions of the concentration profiles and at the locations of maxima and minima in concentrations of the various components. The concentrations at the end-points of each region were identified with the experimental data as listed in Table 3. The concentration derivatives at the end-points of each region were calculated by the *Multi*DiFlux program but were set to zero at each maximum and minimum in concentrations and at the endpoints of the terminal regions, Region 1 and Region 7, as indicated in Table 3. The profiles in Region 3 show appreciable variation in curvature; therefore, Region 3 was further divided into three elements to aid in the interpolation process. The interpolated profiles determined by the method of least squares are shown by the continuous curves in Fig. 3(a) for the individual components.

Profiles of interdiffusion fluxes, $\tilde{J}_i$ versus x, were then calculated on the basis of Eq 3 and are shown in Fig. 3(b). As the variation in molar volume V_m is considered negligible and concentrations are expressed in atom fractions, V_m was taken as 1 in Eq 3 and the flux unit is expressed in atom fraction μm/s. These fluxes can be converted into units of moles/μm^2/s by multiplying with the molar density. The Matano plane was calculated to be at $x = 255$ μm, as marked on Fig. 3(b). Cu developed a zero-flux plane (ZFP) on the α_2 side of the diffusion couple at $x = 243$ μm, as can be seen from the flux profiles shown in Fig. 3(b).

The next step of calculating the ternary interdiffusion coefficients was carried out over selected ranges of composition in the diffusion zone. In general, several choices exist for dividing the diffusion zone into regions and the subsequent calculation of interdiffusion coefficients. The goal here is to select a minimum number of composition ranges and use a minimum number of sets of interdiffusion coefficients necessary for the efficient regeneration of the concentration profiles. Hence, the diffusion zone of the α_2 versus α_7 couple can be divided into two regions, one on either side of the Matano plane. However, in cases where there is a maximum or a minimum near the Matano plane, the location of the maximum or minimum may be used as a convenient dividing section for the diffusion zone. On

Table 3 Compositions and derivatives used to fit the experimental data for α_2 vs. α_7 diffusion couple

	x-location, μm	Composition (atom fraction)			Concentration derivatives, atom fraction/μm		
		C_{Zn}	C_{Ni}	C_{Cu}	C'_{Zn}	C'_{Ni}	C'_{Cu}
x_1	0	0.166	0.097	0.738	0	0	0
x_2	90	0.166	0.097	0.738	0	0	0
x_3	190	0.136	0.097	0.766	-5.8×10^{-5}	0	0
x_4	260	0.117	0.333	0.55	-1.6×10^{-3}	2.2×10^{-3}	-6.1×10^{-4}
x_5	310	0.006	0.422	0.572	-8.8×10^{-4}	9.8×10^{-4}	0
x_6	330	0.0	0.433	0.567	0	3.3×10^{-4}	-3.0×10^{-4}
x_7	380	0.0	0.444	0.556	0	0	0
x_8	500	0.0	0.444	0.556	0	0	0

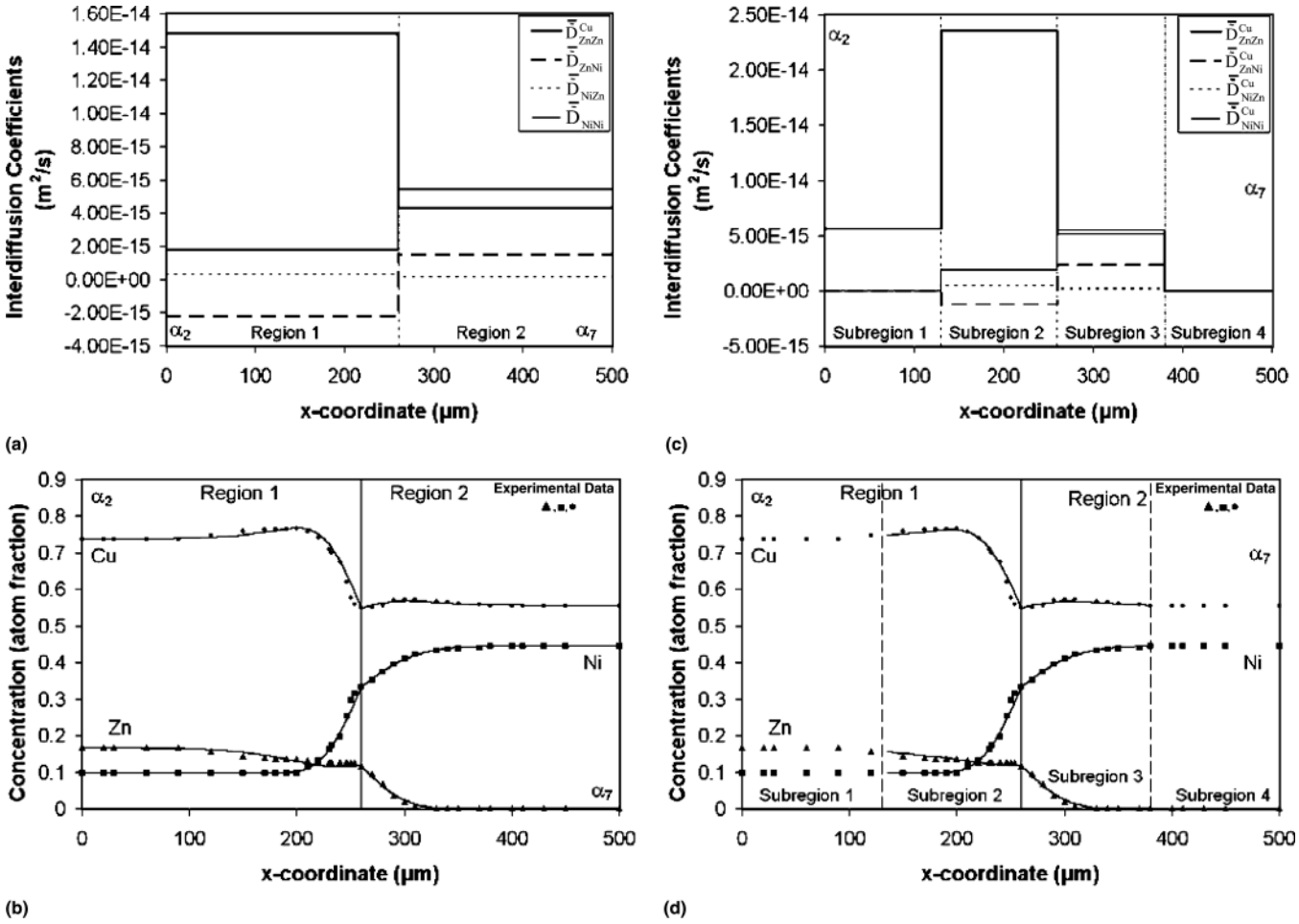

Fig. 4 (a) Interdiffusion coefficients calculated for two regions, 1 and 2, in the diffusion zone for α_2 versus α_7 couple; (b) regenerated concentration profiles using the calculated interdiffusion coefficients; (c) interdiffusion coefficients calculated over four subregions by dividing Region 1 and Region 2 into two subregions; (d) regenerated concentration profiles using the calculated interdiffusion coefficients over subregions 2 and 3

choosing two regions, one on either side of the Cu minimum, two sets of interdiffusion coefficients were calculated by the program; these are shown in Fig. 4(a). These coefficients were then used in Eq 11 and 12 for the regeneration of concentration profiles shown by the solid lines in Fig. 4(b). Thus, the concentration profiles can be satisfactorily regenerated with only two sets of interdiffusion coefficients evaluated over two regions in the diffusion zone.

One may choose to divide each of these two regions further into two subregions to calculate the interdiffusion coefficients over four smaller regions in the diffusion zone. Such four subregions are shown in Fig. 4(c) and 4(d). The interdiffusion coefficients calculated within the smaller subregions 2 and 3 in Fig. 4(c) are now slightly different from those that were calculated as average values over the larger regions of Region 1 and Region 2 in Fig. 4(a). The coefficients calculated for the outer Subregion 1 and Subregion 4 are considered approximate because the concentration profiles in these regions are quite flat and give rise to appreciable errors in setting up Eq. 5 and 9. From the interdiffusion coefficients calculated over Subregions 2 and 3 only, the *Multi*DiFlux program can regenerate the concentration profiles as shown in Fig. 4(d); these profiles are almost identical to those generated in Fig. 4(b) over the same diffusion zone. These observations indicate that the analysis of ternary diffusion couples exhibiting concentration maxima and minima as well as zero-flux planes for the individual components can still be carried out with only a few sets of ternary interdiffusion coefficients determined as averages over selected composition ranges in the diffusion zone. These interdiffusion coefficients may vary slightly with the width or range selected in the diffusion zone but can still generate the profiles in the selected range on the basis of error functions.

The calculation of interdiffusion coefficients may also be carried out over small segments (~/μm) of the diffusion zone to assess their variation with composition. For the α_2 versus α_7 diffusion couple, such calculations are illustrated by dividing its diffusion zone between $x = 100$ and 360 μm into 260 subregions, 1 μm in width, and calculating one set of interdiffusion coefficients for each subregion. Variations of the ternary interdiffusion coefficients over these subregions are shown in Fig. 5(a) and (b). The rise in the value of $\bar{\tilde{D}}^{Cu}_{ZnZn}$ shown in Fig. 5(a) is consistent with the fact that the magnitude of the Zn gradient in the diffusion zone initially increases from the α_2 side of the couple but exhibits a decrease in the vicinity of x of about 200 μm. As the Zn interdiffusion flux increases towards the Matano plane, a rise in $\bar{\tilde{D}}^{Cu}_{ZnZn}$ can compensate for the decrease in the magnitude of the negative Zn gradient on the basis of Eq 7. Similarly, a rise in the magnitude of the negative $\bar{\tilde{D}}^{Cu}_{ZnNi}$ coefficient also helps contribute to an increase in the interdiffusion flux of Zn that is interdiffusing against a positive concentration gradient of Ni.

The flux profiles that were regenerated with the calculated interdiffusion coefficients from Eq 7 are shown in Fig. 5(c). The major difference between the regenerated flux profiles and the original flux profiles shown in Fig. 3(b) is in the vicinity of $x = 200$ μm due to the apparent spike in the value of the coefficient in this region (Fig. 5a). On the whole, the regenerated flux profiles compare very favorably with the original flux profiles and provide support for the methodology used in the development of the *Multi*DiFlux program.

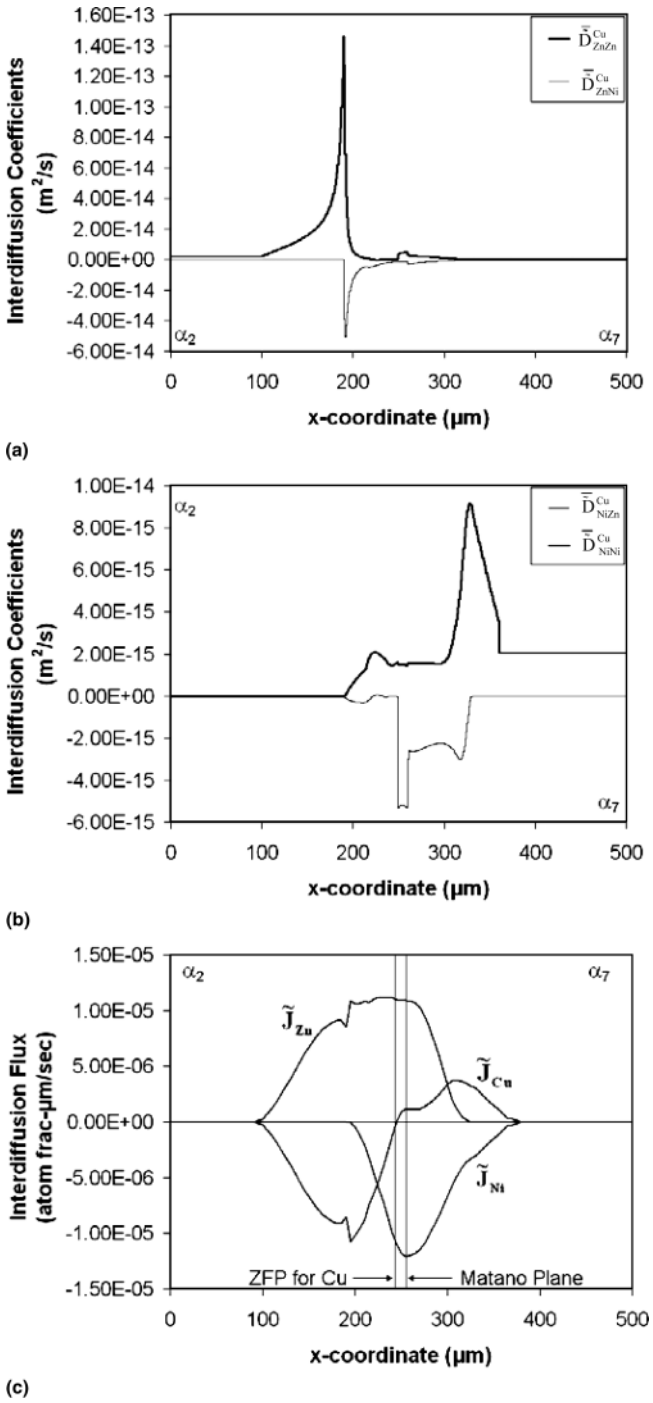

Fig. 5 (a) $\bar{\tilde{D}}^{Cu}_{ZnZn}$ and $\bar{\tilde{D}}^{Cu}_{ZnNi}$ calculated for the α_2 versus α_7 diffusion couple over 260 subregions; (b) $\bar{\tilde{D}}^{Cu}_{NiZn}$ and $\bar{\tilde{D}}^{Cu}_{NiNi}$ calculated for the α_2 versus α_7 diffusion couple over 260 subregions; (c) regeneration of the flux profiles from the calculated interdiffusion coefficients on the basis of Eq 7

7. Comparison of $\tilde{D}^3_{ij}$ from Selected Cu-Ni-Zn Couples

7.1 Pair of Isoactivity Couples with Intersecting Diffusion Paths

Figure 6 shows the diffusion path for the Cu-isoactivity Cu-Ni-Zn diffusion couple, α_2 versus α_7 discussed in Sec. 6. Also shown in Fig. 6 is the diffusion path of another Cu-isoactivity couple, α_{10} versus α_{13} that intersects the path of the couple, α_2 versus α_7. The point of intersection of the diffusion paths corresponds to the composition of 56 at.% Cu, 32 at.% Ni, and 12 at.% Zn. The *Multi*DiFlux program was used to determine ternary interdiffusion coefficients in the region of the common composition, independently from each of the couple pairs, α_2 versus α_7 and α_{10} versus α_{13}.

In Fig. 7 the concentrations profiles are presented for the couples α_2 versus α_7 and α_{10} versus α_{13} identifying the locations of the section of the common composition for each couple. The profiles of the calculated interdiffusion fluxes for both couples are also included in Fig. 7. Similar to the α_2 versus α_7 couple, the couple α_{10} versus α_{13}, also exhibits two relative maxima in Cu concentration, one on either side of the Matano plane and a relative minimum in Cu concentration. Also, both couples develop a zero-flux plane (ZFP) for Cu, as can be seen from the flux profiles shown in Fig. 7(b) and (d).

With the aid of the *Multi*DiFlux program, interdiffusion coefficients were calculated from each couple over a region of the diffusion zone covering 1 μm on either side of the section of common composition. In addition, interdiffusion coefficients were also evaluated at the common composition of the two couples by employing the Boltzmann-Matano analysis.[1] All these calculated coefficients are presented in Table 4. The sets of interdiffusion coefficients calculated from each of the couple pairs compare very favorably and the difference between the individual coefficients ranged between 7 and 27%. These coefficients also compare favorably with those calculated by the Boltzmann-Matano analysis with the difference between the coefficients ranging between 2 and 39%. There does appear to be some error compensation that occurs when the interdiffusion coefficients are calculated. For example, the difference between the main coefficient $\tilde{D}^{Cu}_{ZnZn}$ calculated by the *Multi*DiFlux program and the Boltzmann-Matano method for the couple α_2 versus α_7 is 2%. The complimenting cross coefficient, $\tilde{D}^{Cu}_{ZnNi}$ differs by 21%. It has been observed that when one coefficient, either main or cross, is very close to an expected value, in this case the expected values have been determined by the Boltzmann-Matano method, the complementing coefficient often differs from its expected value by a larger amount. Despite this error compensation, the calculations performed by the MultiDiFlux program indicate consistency in the application of the program, as comparable results are obtained at the compositional point of intersection of the couple pair.

7.2 Pair of Isoactivity Couples with Similar Segments of Their Diffusion Paths

In Fig. 8 the diffusion paths are presented for two Cu-isoactivity couples, α_3 versus α_{15} and α_3 versus α_{18}. The diffusion paths of these couples exhibit similarly oriented and overlapping path segments over the Cu concentration ranging between 51 and 59 at.%, as marked in Fig. 8. Based on the analysis of these couples by the *Multi*Diflux program, the concentration and interdiffusion flux profiles for the α_3 versus α_{15} couple are presented in Fig. 9(a) and (b), respectively, and Fig. 9(c) and (d) show the concentration and interdiffusion flux profiles for the couple, α_3 versus α_{18}.

The α_3 versus α_{15} diffusion couple shows a relative maximum for Cu on the α_3 side of the Matano plane, and the α_3 versus α_{18} couple shows a Cu maximum on either side of the Matano plane. Both couples develop a zero-flux plane for Cu. Also, both couples exhibit a maximum in Zn concentration in the vicinity of the Matano plane.

Interdiffusion coefficients were calculated by the *Multi*DiFlux program from each of the couple pairs over the

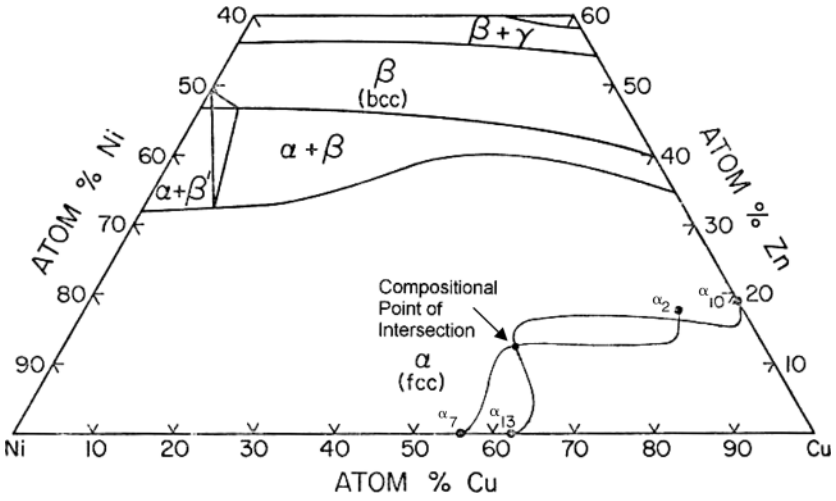

Fig. 6 Diffusion paths for the α_2 versus α_7 and the α_{10} versus α_{13} diffusion couples intersecting at the common composition of 56 at.% Cu, 32 at.% Ni, and 12 at.% Zn. The couples were annealed at 775 °C for two days.[4]

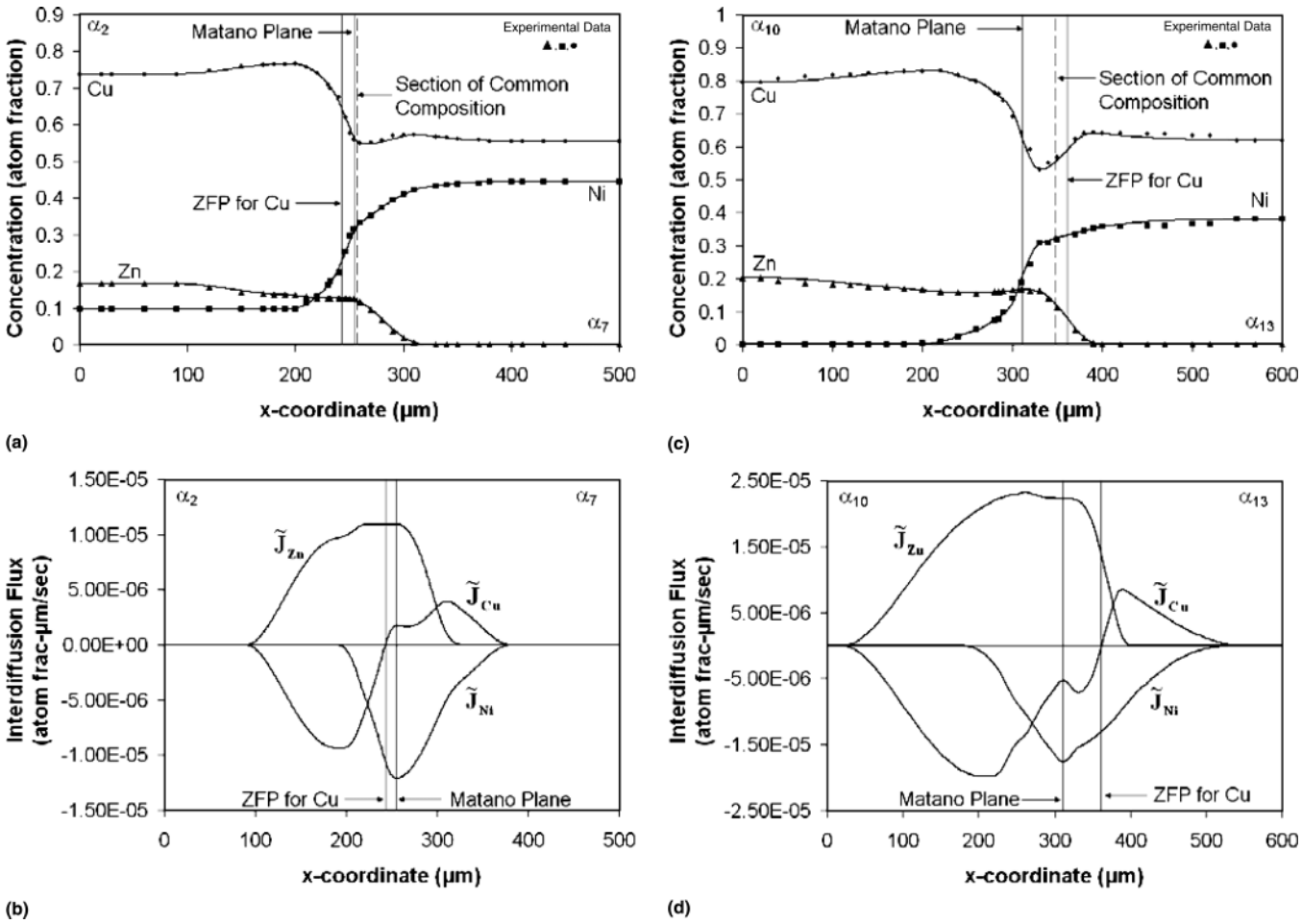

Fig. 7 (a) Concentration profiles and (b) the calculated interdiffusion flux profiles for the α_2 versus α_7 diffusion couple; (c) concentration profiles and (d) the calculated interdiffusion flux profiles for the α_{10} versus α_{13} diffusion couple

Table 4 Interdiffusion coefficients calculated for selected diffusion couples

Couples	Composition range (atom fraction)			Analysis by:	Interdiffusion coefficients $\bar{\tilde{D}}_{ij}^{Cu}$ ($\times 10^{-14}$ m^2/s)			
	Cu	Ni	Zn		$\bar{\tilde{D}}_{ZnZn}^{Cu}$	$\bar{\tilde{D}}_{ZnNi}^{Cu}$	$\bar{\tilde{D}}_{NiZn}^{Cu}$	$\bar{\tilde{D}}_{NiNi}^{Cu}$
Intersection couples								
α_2 vs. α_7	0.56-0.55	0.32-0.33	0.12-0.12	*Multi*DiFlux	0.48	–0.13	–0.52	0.15
α_{10} vs. α_{13}	0.56-0.56	0.32-0.32	0.12-0.12	*Multi*DiFlux	0.57	–0.14	–0.43	0.11
Boltzmann-Matano with:								
α_2 vs. α_7	0.56	0.32	0.12	Boltzmann-Matano	0.58	–0.11	–0.41	0.18
α_{10} vs. α_{13}	…	…	…	…	…	…	…	…
Couples with similar diffusion paths								
α_3 vs. α_{18}	0.59-0.51	0.18-0.26	0.22-0.23	*Multi*DiFlux	13.9	–2.4	–8.0	1.6
α_3 vs. α_{15}	0.59-0.52	0.19-0.25	0.22-0.22	*Multi*DiFlux	12.3	–1.6	–8.0	1.4

overlapping path segments shown in Fig. 8. The composition ranges corresponding to these segments are identified on the concentration profiles of the two couples presented in Fig. 9(a) and (c). The ternary interdiffusion coefficients calculated over these composition ranges from the individual couples are presented in Table 4. It is apparent that these sets of interdiffusion coefficients compare very favorably and that the difference between the individual coefficients from the two couples was between 0 and 33%. Hence, the *Multi*DiFlux interdiffusion calculations show consistency and provide comparable results for similar diffusion path segments exhibited by different diffusion couples.

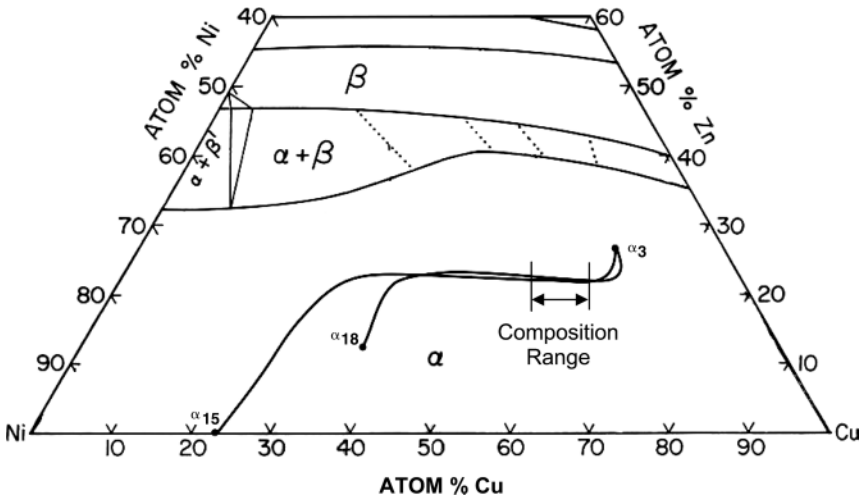

Fig. 8 Diffusion paths of the α_3 versus α_{15} and the α_3 versus α_{18} diffusion couples annealed at 775 °C for two days[4]; the composition range over which interdiffusion coefficients were calculated is marked on the phase diagram

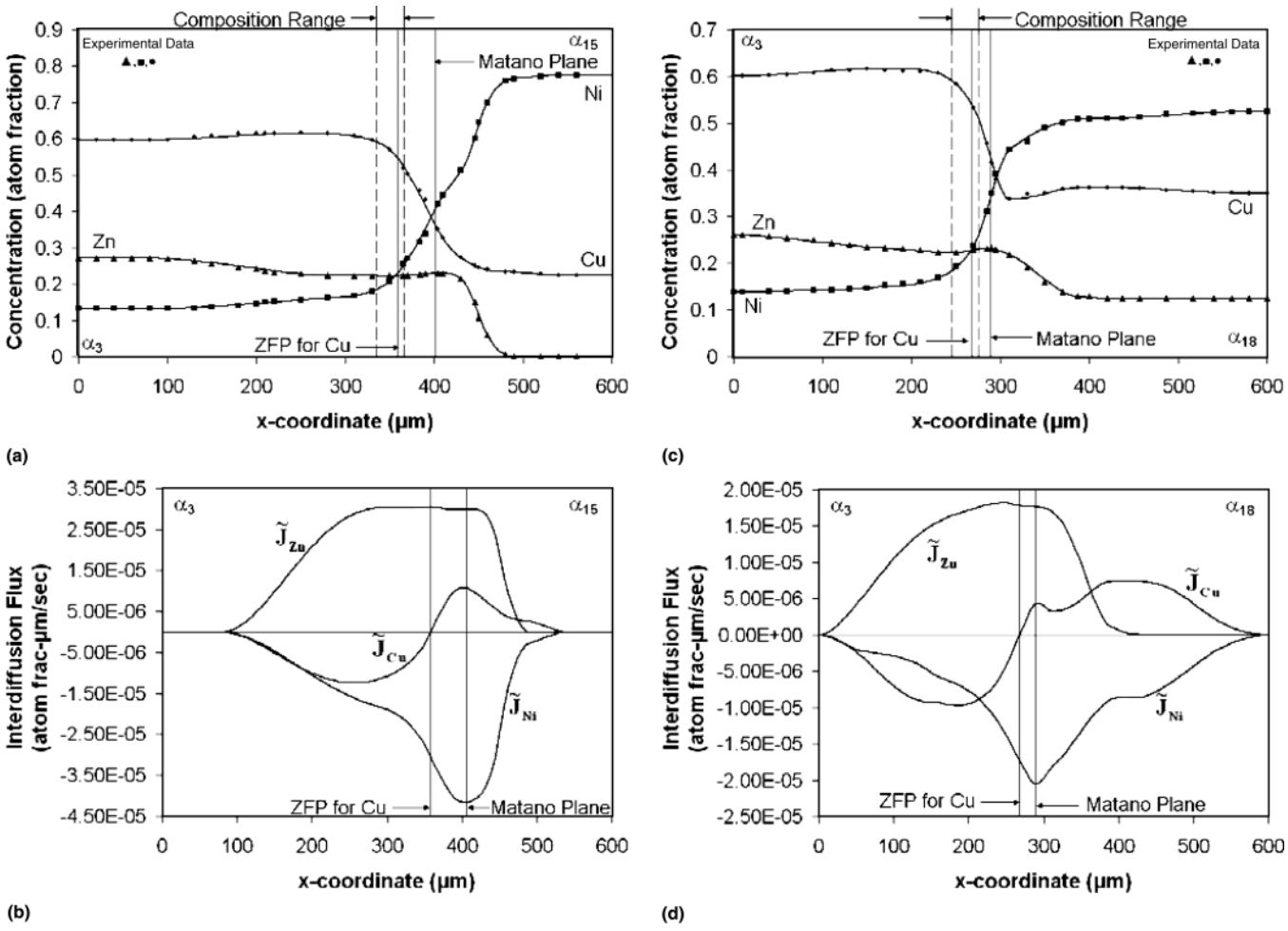

Fig. 9 (a) Concentration profiles and (b) the corresponding interdiffusion flux profiles for the α_3 versus α_{15} diffusion couple; (c) concentration profiles and (d) corresponding interdiffusion flux profiles for the α_3 versus α_{18} diffusion couple

8. Summary

Two pairs of ternary Cu-Ni-Zn diffusion couples were analyzed for interdiffusion fluxes, zero-flux planes, and interdiffusion coefficients directly from concentration profiles. The determination of the interdiffusion coefficients was based on an integration of interdiffusion fluxes over selected concentration ranges within the diffusion zone. The first pair of couples was characterized by intersecting diffusion paths. At the compositional point of intersection, ternary interdiffusion coefficients were calculated from each of the couples, as well as by the Boltzmann-Matano method. The interdiffusion coefficients calculated from the individual couples agreed with each other and with those calculated by the Boltzmann-Matano analysis. The second set of diffusion couples was characterized with similar and overlapping diffusion path segments. Interdiffusion coefficients calculated as average values over the overlapping path segments from the individual couples also agreed with each other. All calculations were carried out with the aid of a freely downloadable computer program called *Multi*DiFlux developed by Dayananda and Ram-Mohan as a teaching and research tool. The program was tested for interdiffusion calculations with a test couple and its use was illustrated with an experimental diffusion couple. The interdiffusion coefficients calculated by the program were also used to regenerate the concentration and flux profiles for a check of the consistency in the calculations.

Acknowledgment

This work was supported by the National Science Foundation under Grant No. DMR-0304777.

References

1. J.S. Kirkaldy and D.J. Young, *Diffusion in the Condensed State,* The Institute of Metals, London, UK, 1987, p 226-272
2. M.A. Dayananda and Y.H. Sohn, A New Analysis for the Determination of Ternary Interdiffusion Coefficients from a Single Diffusion Couple, *Metall. and Mater. Trans. A,* Vol 30A (No. 3), 1999, p 535-543
3. M.A. Dayananda and C.W. Kim, Zero-Flux Planes and Flux Reversals in Cu-Ni-Zn Diffusion Couples, *Metall. Trans. A,* Vol 10A (No. 9), 1979, p 1333-1339
4. C.W. Kim and M.A. Dayananda, Zero-Flux Planes and Flux Reversals in the Cu-Ni-Zn System at 775 degree C, *Metall. Trans. A,* Vol 15A (No. 4), 1984, p 649-659
5. M.A. Dayananda and L.R. Ram-Mohan, *Multi*DiFlux https://engineering.purdue.edu/MSE/Fac_Staff/Faculty/dayananda.wshtml, 2005, Purdue University
6. M.A. Dayananda, Analysis of Concentration Profiles for Fluxes, Diffusion Depths, and Zero-Flux Planes in Multicomponent Diffusion, *Metall. Trans. A,* Vol 14A (No. 9), 1983, p 1851-1858
7. M.A. Dayananda, Analysis of Multicomponent Diffusion Couples for Interdiffusion Fluxes and Interdiffusion Coefficients, *J. Phase Equilibria Diffusion,* Vol 26 (No. 5), 2005, p 441-446
8. R.D. Sisson, Jr. and M.A. Dayananda, Diffusional and Thermodynamic Interactions in the Cu-Ni-Zn System at 775 °C, *Metall. Trans.,* Vol 8A, 1977, p 1849-1856
9. C.W. Kim and M.A. Dayananda, Identification of Zero-Flux Planes and Flux Reversals in Several Studies of Ternary Diffusion, *Metall. Trans. A,* Vol 14A (No. 5), 1983, p 857-864
10. G.L. Kehl, *The Principles of Metallographic Laboratory Practice,* McGraw-Hill, NY, 1949, p 420
11. L. Onsager, Reciprocal Relations in Irreversible Processes I, *Phys. Rev.,* Vol 37, 1931, p 405-425
12. L.R. Ram-Mohan, *Finite Element and Boundary Element Applications to Quantum Mechanics*, Oxford University Press, Oxford, UK, 2002, p 63-81